International Journal of Research in Engineering, Science and Management
Volume 8, Issue 10, October 2025
https://www.ijresm.com | ISSN (Online): 2581-5792

Development and Characterization of Magadiitic Aluminosilcate Nanozeolite Adsorbent Using Magadi Salt from Lake Magadi, Kenya

Janes Bochaberi Omoko[1*], Njagi Njomo[2], Deborah A. Abong'o[3], Dickson M. Andala[4]
[1,2,3]*Department of Chemistry, Faculty of Science & Technology, University of Nairobi, Nairobi, Kenya*
[4]*Department of Chemistry, Multimedia University, Nairobi, Kenya*

***Abstract*: A Magadiitic Aluminosilicate nanozeolite (AP-05-02) was developed from Lake Magadi's Magadi salt, Kenya, as a cost-effective water adsorbent, confirmed by XRD, EDX, FT-IR, XRF and SEM analysis to possess a porous aluminosilicate structure for water pollution reduction. Its aluminosilicate nature was verified by FT-IR analysis showing characteristic framework vibrations, and its chemical composition determined by XRF, revealed high SiO_2 (77.282 %), Al_2O_3 (12.400 %), and K_2O (7.469 %) contents, while SEM showed a rough surface with agglomerated particles and interconnected pores. The provided data described a nonparticulate material (around 21 nm) with a well-developed porous structure, characterized by a high surface area (285.88 m^2/g BET, 895.80 m^2/g, Langmuir), signifying total pore volume (0.231 cm^3/g), notably high volume of micropores (0.242 cm^3/g) and ultra-micropores (0.044 cm^3/g). The pore distributions, including ultra-micropores suitable for molecular sieving and mesoporous average pore diameter (32.3–78.3 Å) adding to the material versatile adsorption capabilities and further will enhance its functionality in specific separation application.**

***Keywords*: adsorbent, aluminosilcate, magadiitic, microporous, nanoparticle, nanozeolite.**

1. Introduction

Zeolites have a three-dimensional structure composed of interlinked silica (SiO_4) and alumina (AlO_4) tetrahedral [1]. This structure creates pores of defined sizes that range from 0.3 - 1.0 nm spaces [2], [3]. The pore size of zeolites allows them to selectively adsorb molecules based on size and shape [4]. Zeolites can be found naturally occurring or synthesized in a laboratory, they can be used for water softening and the removal of pollutants from wastewater [5]. The structure of zeolites has surface-active centers, which gives them good adsorption and catalytic activity. For this reason, this study focused on developing magadiitic aluminosilcate nanozeolite using Magadi salt from Lake Magadi, Kenya, as an adsorbent. The developed adsorbent was characterized, its structure, morphology, surface area, and chemical composition were determined. The development of a low-cost effective adsorbent is important as an alternative cheap method for reducing water pollutants.

2. Literature Review

Zeolites are stable, high-melting points (<1000 °C) [6] crystalline aluminosilicate solids composed of silicon, aluminium and oxygen [7] with a three -dimensional framework of shared tetrahedral ($[AlO_4]^{5-}$ and $[SiO_4]^{4-}$) [8] [9]. This structure creates a network of interconnected void and open spaces that enables zeolites to function as adsorbents, catalysts and ion exchangers [10]. In the zeolite structure, the typical bond lengths for Si-O is approximately 1.6 Å, O-O is 3.07 Å and Si-Si is 2.63 Å representing the average distance between these atoms within the crystalline framework of corner-sharing SiO_4 and AlO_4 tetrahedral [11]. Zeolite cages are formed by connecting pore opening varying approximately 0.3-1.0 nm in tetrahedral structure [3]. The negative charge in the cage structure are neutralized by cations. The unique structural features of zeolites contribute significantly to their diverse applications. The presence of channels and chambers within the zeolite framework provides them with exceptional physicochemical properties [12]. The size of the pores in zeolites is a fundamental characteristic that governs their structural, chemical, and physical properties, allowing for the design of materials tailored for specific applications in catalysis, adsorption, and ion exchange [13]. This, as it allows zeolites to separate molecules based on size and shape, permitting smaller molecules to enter the pores while excluding larger ones. This property is vital in processes like gas separation and purification, as well as in environmental applications such as the removal of specific pollutants from wastewater, where pore size can enhance the adsorption of target contaminants [14]. Furthermore, pore size dictates the mobility and selective exchange of ions, a key factor in applications like water softening where smaller pores might preferentially retain certain cations. The interaction of zeolites with water and organic solvents, mechanical stability, and thermal stability are also highly dependent on pore characteristics [15]. Therefore, the characterization of a newly developed adsorbent's structure, morphology, and surface area is essential for understanding and optimizing its performance.

*Corresponding author: omokojanes@gmail.com

3. Materials and Methods

The study area was Lake Magadi which is the southernmost lake in the Kenyan Rift Valley, lying in catchment of faulted volcanic rocks. It lies at 1° 52’ 0’’ S and 36° 16’ 60’’E (Figure 1). It experiences a semi-arid climate with a bimodal rainfall pattern of 460 mm of rainfall annually, with a mean of 50 mm. The lake has surface area of approximately 75,00 km^2 and a length of 32 km. Minerals found in Lake Magadi include Cherts like alligator skin type typical chert type rock, Cauliform cherts, magadiite, makatite and Kenyaite [16]. This study focused on Magadiitic salts samples collected from five sampling sites shown in Table 1.

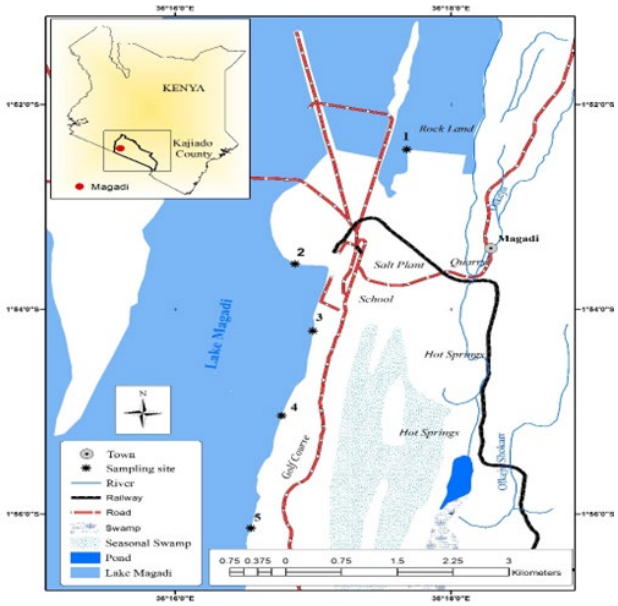

Fig. 1. A map of sampling sites at lake Magadi, Kenya

The study involved several key steps, starting with the collection of magadiitic salt samples from Lake Magadi in Kenya (Figure 1). These samples were collected from five different sites on the lake's shore (Table 1), specifically targeting relatively bare surface deposits areas. The five collected samples had similar chemical properties. Therefore, the samples were mixed together to form a composite sample SA-02, this composition strongly indicated that sample SA-02 was not a zeolite but likely represented a non-zeolitic material, possibly a NaCl-rich deposit or carbonaceous contaminant, which was used for subsequent experimental analysis. The design begun with the preparation of two separate solutions. First, an aluminium sulphate solution was made by dissolving 666 g of aluminium sulphate octadecahydrate in 500 mL of distilled deionized water, which was then diluted to a final volume of one litre using distilled deionized water. Three different one-litre solutions of a magadiitic salt were prepared by dissolving 500 g of crushed sample SA-02 in warm distilled deionized water. A reaction was initiated by adding 600 mL of the aluminium sulphate solution, containing 133.5 g/L of the salt, to each of the three different one-litre solutions of magadiitic solution, which resulted in a solution with a pH between 4.7 and 7.7. This mixture was then divided into three equal one-litre portions. Different amounts of the aluminium sulphate solution were added to each portion to induce precipitation: 50 mL was added to the first portion to yield sample SA-03, 100 mL to the second for sample AP-05-01, and 200 mL to the third for sample AP-05-02. The resulting precipitated material were identified as Magadiitic aluminosilicate nanozeolites. Following precipitation, these materials were filtered using a Lab Recessed Chamber Filter Press and three different samples SA-03, AP-05-01 and AP-05-02 were produced and washed with distilled deionized water to remove impurities such as unreacted metal silicate and sodium sulphate. The filtered cakes were then dried using a flash dryer at an inlet temperature of 350°C and an outlet temperature of 120°C. Finally, the dried Magadiitic aluminosilicate materials were ground in a ball mill to achieve an average particle size of 1-15µm, and the resulting final product, magadiitic aluminosilicate nanozeolite, was stored for future laboratory analysis. Samples Ap-05-01, Ap-05-02, and SA-03 all showed strong matches to reference peaks from the Inorganic Crystal Structure Database (ICSD) specifically within the ranges of 20.7°–20.9°, 26.6°–26.9°, and 36.4°–36.6° respectively, thereby confirming the presence of crystalline quartz [17]. The precision of this peak alignment, within ±0.3° 2θ, supported the phase purity of SiO_2 in these three samples [18]. In conclusion, the XRD analysis successfully identified mixed α/γ-Al_2O_3 phases in samples Ap-05-01 and SA-03, pure γ-Al_2O_3 in sample AP-05-02, and crystalline SiO_2 in the three samples. However, potassium (K) was only present in AP-05-02 (3.5 wt %), which could suggest the presence of K-feldspar or mica minerals [19]. Sample AP-05-02 was chosen and taken through extensive characterization using several techniques to determine its properties. X-ray fluorescence (XRF) was used to determine the elemental composition of the sample. Fourier-transform infrared spectroscopy (FT-IR) was used to identify functional groups and structural components. Brunauer-Emmett-Teller (BET) analysis was conducted to measure the surface area and pore characteristics. X-ray diffraction (XRD) analysis was used to identify the crystalline phases present in the sample. Scanning electron microscopy with energy-dispersive X-ray spectroscopy (SEM/EDX) was utilized to observe the morphology and determine the elemental composition at the microscale

Table 1
Description of the sampling sites

Site	Local name	Coordinates		Height above the sea levels (m)	Human activities
		Latitude	Longitude		
1	Magadi	1° 52' 26.78"S	36° 17' 39.31" E	601	Salt harvesting
2	Magadi	1° 53' 34.24" S	36° 16' 52.19" E	601	Salt harvesting
3	Magadi	1° 54' 34.93"S	36° 17' 1.83"E	601	Salt harvesting
4	Magadi	1°55' 2.05" S	36° 16' 46.30" E	601	Salt harvesting
5	Magadi	1°56' 7.86" S	36° 16' 32.11"E	601	Salt harvesting

4. Results and Discussion

A. X-Ray Fluorescence (XRF)

X-ray fluorescence (XRF) technology is analytical technique used to determine the elemental composition of materials. This technology leverages the emission properties of materials to interpret their chemical content [20]. The XRF analysis (Table 2) revealed the elemental composition of AP-05-02, showing that it contained Al_2O_3 (12.400 %), SiO_2 (77.282 %) and P_2O_5 (0.132 %). It also contained trace amounts of other elements like titanium (Ti) 0.332 %, iron (Fe) 0.172 %, and potassium oxide (KO) 7.469 %. The chlorine content was low, at 0.884 %.

Table 2
X-ray fluorescence composition of magadiitic aluminosilicate nanozeolite

Element	AP-05-02	+/-[*3]
Al_2O_3 %	12.400	0.547
SiO_2 %	77.282	0.701
P_2O_5 %	0.132	0.055
Cl %	0.884	0.016
K_2O %	7.469	0.051
CaO %	0.438	0.018
Ti %	0.332	0.009
Fe %	0.172	0.008
Nb %	0.008	0.002

B. Fourier-Transform Infrared Spectroscopy (FT-IR)

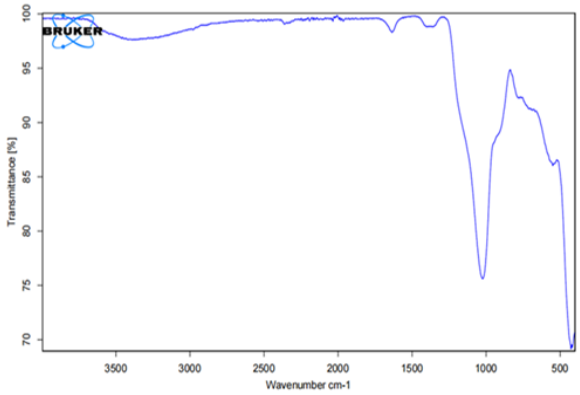

Fig. 2. FT-IR spectra of sample AP-05-02

Infrared spectra of the magadiitic aluminosilcate nanozeolite sample AP-05-02 were scanned in the mid and far (4000-250 cm^{-1}) infrared regions to generate distinct peaks as illustrated by Figure 2. FT-IR analysis showed that AP-05-02 exhibited a peak around 1603 cm^{-1}, which was attributed to H-O-H bending vibrations, indicating the presence of adsorbed water [21]. A prominent peak was also observed at 1168 cm^{-1}, which corresponded to the asymmetric Si-O stretching vibrations within the internal tetrahedra of the magadiitic aluminosilicate framework, confirming the zeolitic nature of the sample. Additionally, peaks in the 853 cm^{-1} and 446 cm^{-1} regions were attributed to Al-O stretching and Si-O-Si bending, respectively, which further confirmed the presence of magadiitic aluminosilicate nanozeolite framework.

C. Brunauer-Emmett-Teller (BET) Analysis

BET analysis determined the surface area and pore characteristics of AP-05-02. The BET surface area was measured to be 285.8763 m^2/g, while the Langmuir surface area was 895.8028 m^2/g. The t-plot micro pore area was calculated to be 110.7999 m^2/g. The analysis revealed a single point adsorption total pore volume of 0.230911 cm^3/g and a single point desorption total pore volume of 0.242466 cm^3/g. The average pore diameters ranged between 32.309 Å and 78.342 Å depending on the calculation method. The median pore width, as determined by the Horvath-Kawazoe method, was 6.935 Å. BET isotherm log plot was shown by Figure 3, BET surface area plot Figure 4, and Langmuir surface area plot Figure 5.

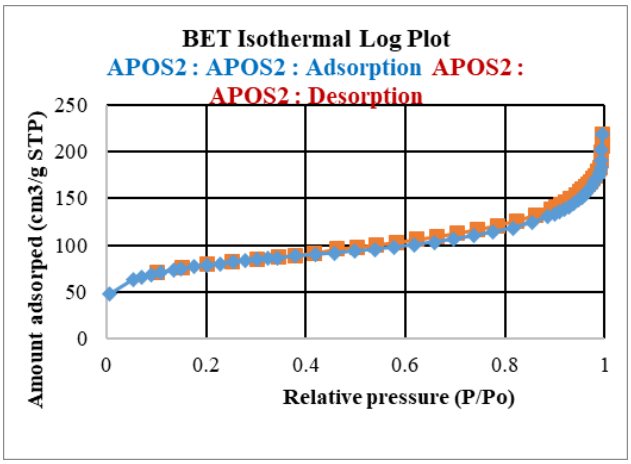

Fig. 3. BET isotherm log plot

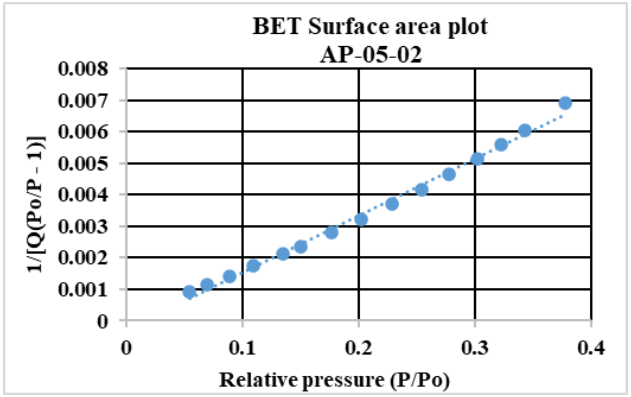

Fig. 4. BET Surface area plot

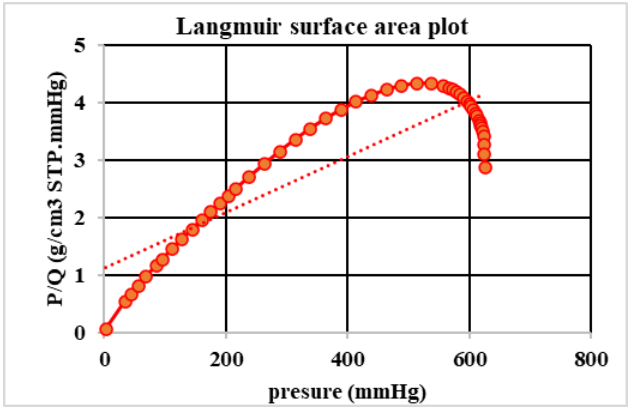

Fig. 5. Langmuir surface area plot

D. X-Ray Diffraction (XRD) Analysis

XRD analysis (Figure 6) revealed peaks at 21.3°, 30.6°, and 36.95°. These peaks align closely with the reference peaks for

gamma-Al_2O_3, suggesting that sample AP-05-02 predominantly contained the gamma form of aluminium oxide**.** Additionally, XRD peaks at 20.89°, 26.7°, and 37.08° closely matched the reference peaks for SiO_2, indicating the presence of silicon dioxide (Figure 6).

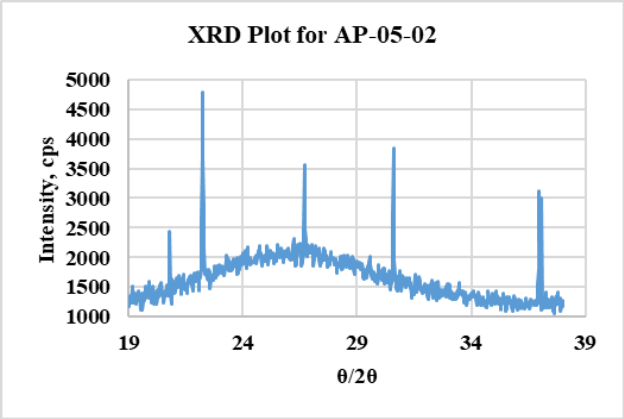

Fig. 6. XRD plot for AP-05-02

E. Scanning Electron Microscopy (SEM)

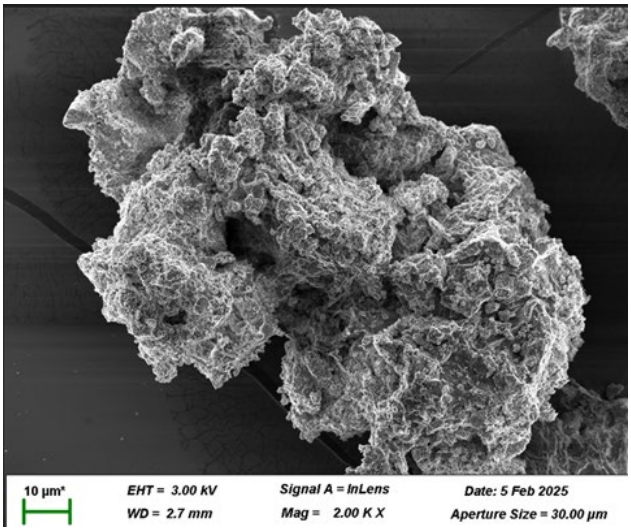

Fig. 7. Secondary electron image of sample AP-05-02

The SEM image for sample AP-05-02 (Figure 7) showed that the particles were unevenly sized. The crystals were dense aggregates of irregular shapes.

F. Energy-Dispersive X-Ray Spectroscopy (EDX)

The elemental composition of sample AP-05-02, as determined by weight percentage (wt %) (Figure 8), revealed key components. Oxygen (O) constituted a significant portion at 43.4 %, indicating the presence of oxides or other oxygen-containing compounds. Carbon (C) was also a major element, accounting for 23.8 %, which could be related to organic matter or carbonate compounds. Silicon (Si) was present at 23.1 %, suggesting the existence of silica-based materials or silicates. Aluminium (Al) was found in a smaller amount, 4.4 %, potentially indicating aluminosilicate minerals. Minor elements included sodium (Na) at 1.0 %, sulphur (S) was 0.3 %, and chlorine (Cl) at 0.5 %. Potassium (K) was also detected at 3.5 %. From the elemental composition computation, the sample AP-05-02 has a chemical formula of $KNaAl_4Si_{23}C_{24}O_{43}$**.**

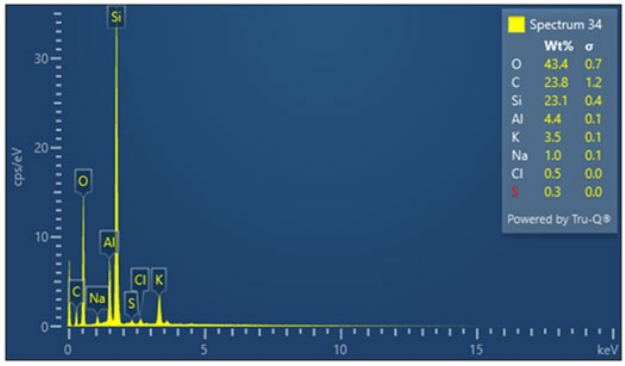

Fig. 8. EDX data for sample AP-05-02

5. Conclusion

The study aimed at developing a low-cost adsorbent from magadiitic salt found in Lake Magadi, Kenya, and the characterization techniques employed provided valuable insights into the properties of the synthesized magadiitic aluminosilicate (Sample AP-05-02). XRF analysis confirmed the presence of significant amounts of Al_2O_3 (12.400 %) and SiO_2 (77.282 %), demonstrating the successful development of an aluminosilicate material. FT-IR analysis further validated the formation of a zeolitic structure, identifying peaks indicative of adsorbed water, Si-O stretching vibrations, and the aluminosilicate framework. BET analysis revealed a BET surface area of 285.8763 m^2/g and a Langmuir surface area of 895.8028 m^2/g, with pore diameters ranging from 32.309 Å to 78.342 Å, indicating the microporous nature of the material. XRD analysis identified peaks corresponding to gamma-Al_2O_3 and SiO_2, confirming their presence in the synthesized material. The SEM images showed unevenly size particles and crystals were dense aggregates of irregular shapes. The EDX analysis displayed an aggregated morphology of smaller nanoparticles and exhibit compositional variations with heavy element incorporation and determined the elemental composition, leading to the chemical formula $KNaAl_4Si_{23}C_{24}O_{43}$. Overall, the characterization results confirmed that the synthesized magadiitic aluminosilicate nanozeolite exhibited the characteristics of a microporous material with a high surface area, suggesting its potential for high cation exchange and adsorption capacities, which aligns with the study's objective of developing a cost-effective adsorbent for reducing water pollution. In conclusion, while the study offers a detailed investigation into magadiitic aluminosilcate nanozeolites for adsorption, its findings are constrained by material specificity, pollutant range, and lab-scale conditions. Future research is recommended to explore scalability, real-world application, and broader pollutant removal efficiency to enhance practical adoption.

Acknowledgement

The authors would like to acknowledge Dr. Pierre Kalenga Mubiayi and the Technicians, at the University of the Witwatersrand, School of Chemistry for their immense support

in the characterization process. Also, thank the Technicians at the Department of Mines and Geology (Madini House), Nairobi for their support during XRF characterization. Lastly, thank the staff at the Department of Chemistry of the University of Nairobi where this analysis was conducted.

References

[1] Dong-Mei G., Qing-Da A., Zuo-Yi X., Shang-Ru Z., Dong-Jiang Y. (2018). Efficient removal of Pb (II), Cr (VI) and organic dyes by polydopamine modified chitosan aerogels. *Carbohydrate Polymers*, 202: pp. 306-314.

[2] Kar Y. H., Jasmine M. C. C., Meng N. C., Bo J., Christopher S., Phaik E. P., Rupak A., (2016). Evaluation of physicochemical methods in enhancing the adsorption performance of natural zeolite as low-cost adsorbent of methylene blue dye from wastewater. *Journal of Cleaner Production*, 118: pp. 197-209.

[3] Fantini, Riccardo & Argenziano, Monica & Cavalli, Roberta & Arletti, Rossella & Mino, Lorenzo) (2024). Zeofilters for potentially innovative sunscreen products: formulation, stability and spectroscopic studies. *Journal of Photochemistry and Photobiology A: Chemistry*, 452: pp. 115585.

[4] De Souza, V.C.; Villarroel-Rocha, J.; De Araújo, M.J.G.; Sapag, K.; Pergher, S.B.C. (2018). Basic treatment in natural clinoptilolite for improvement of physicochemical properties. *Minerals*, 8: pp. 595.

[5] Justyna Szerement, Alicia Szatanik – Kloc, Ranata Jarosz, Tomasz Bajda, Monika Mierzwa– Hersztek. (2021). Contemporally appilications of natural and synthetic zeolites from fly ash in agriculture and environmental protection. *Journal of cleaner production*, 311, pp. 127-461.

[6] Bailey S.E., Olin T.J., Bricka R.M. & Adrian D.D., (1999). A review of potentially low costs sorbents for heavy metals. *Water Research*, 33: pp. 2469-2479.

[7] Hallvard F. S., Erik T. H. & ThorMejdell, (2011). Carbon dioxide capture by absorption, challenges and possibilities. *Chemical Engineering Journal*, 171: pp. 718-724.

[8] Ionel H., Adriana B., Maurusa-Elena I., Viorica D., (2017). The removal of Basic Blue 41 textile dye from aqueous solution by adsorption onto natural zeolitic tuff: Kinetics and thermodynamics. *Process Safety and Environmental Protection*, 105: pp. 274-287.

[9] Boyd G. E., Adamson A. W. & Myers L. S. (1947). The Exchange Adsorption of Ions from Aqueous Solutions by Organic Zeolites. *Journal of the American Chemical Society, 69*: pp. 2836-2848.

[10] Kar Y. H., Jasmine M. C. C., Meng N. C., Bo J., Christopher S., Phaik E. P., Rupak A., (2016). Evaluation of physicochemical methods in enhancing the adsorption performance of natural zeolite as low-cost adsorbent of methylene blue dye from wastewater. *Journal of Cleaner Production*, 118: pp. 197-209.

[11] Breck D. W., (1974). Zeolite Molecular Sieves: Structure, Chemistry and Use. London: John Wiley and sons, p. 4.

[12] Ryan K. J., Ray C. G., Ahmad N., Drew W. L., Lagunoff M., Pottinger P., Reller L. B. & Sterling C. R., (2014). "Pathogenesis of Bacterial Infections". *Sherris Medical Microbiology New York: McGraw Hill Education,* 6:391-406.

[13] De Souza V. C., Villarroel-Rocha J., De Araújo M.J.G., Sapag K., Pergher S.B.C. (2018). Basic treatment in natural clinoptilolite for improvement of physicochemical properties. *Minerals*, 8: pp. 595.

[14] Ustyna S., Alicia S., Ranata J., Tomasz B. & Monika M., 2021. Contemporally applications of natural and synthetic zeolites from fly ash in agriculture and environmental protection. *Journal of cleaner production,* 311: pp. 127461.

[15] Amine B. M., Amir A., Ludovic P., Jean D. T. & Thomas B., (2017). New Approach to the Acidity Characterization of Pristine Zeolite Crystals by Ethylene Using Reversed-Flow Inverse Gas Chromatography (RF-IGC). *The Journal of Physical Chemistry,* 121: pp. 2738-2747.

[16] Eugster H.P. (1969). Inorganic bedded cherts from the Magadi area, Kenya. *Mineralogy & Petrology*: 22: pp. 1-31.

[17] Jenkins, R., & Snyder, R. L. (1996). *Introduction to X-ray Powder Diffractometry*. Wiley.

[18] Smith, D. K., Johnson, A. B., & Williams, C. D. (2018). *X-ray diffraction and the identification and analysis of clay minerals* (3rd ed.). Oxford University Press.

[19] Klein C. & Dutrow B. (2007). *The 23rd edition of the manual of mineral science* (after James D. Dana). John Wiley & Sons.

[20] Nygård K. & Hämäläinen, K. & Manninen, Seppo & Jalas, P. & Ruottinen, J. P. (2004). Quantitative thickness determination using X-ray fluorescence: *Application to multiple layers. X-Ray Spectrometry*, 33: pp. 354-359.

[21] Madejová, J. FTIR techniques in clay mineral studies. *Vibrational Spectroscopy,* 31(1), pp. 1-10, 2003.